Research in Earthquake Physics, Forecasting, and Simulation-Based Probabilistic Hazard Assessment at the University of California, Davis

http://quakesim.jpl.nasa.gov

Woodblock Print, from "Thirty-Six Views of Mt. Fuji", by K. Hokusai, ca. 1830

Donald L Turcotte

University of California, Davis

in Collaboration with the QuakeSim Team

Presented at the UJNR Meeting
Asilomar, CA, October 14, 2004

Collaborators

Andrea Donnellan, Division of Earth and Space Science, JPL

Geoffrey Fox, Dept. of Computer Science, University of Indiana

Robert Granat ,Data Understanding Systems Group, JPL

Lisa Grant, Dept. of Environmental Science, University of California, Irvine

James Holliday, Dept. of Physics and CSE, University of California, Davis

Peggy Li, Parallel Applications Technologies Group, JPL

Bill Klein, Dept. of Physics, Boston Univ.; and CNLS, LANL

Greg Lyzenga, Dept. of Physics, Harvey Mudd College

Jorge Martins, Universidad Fluminense, Niteroi, Brazil

Dennis McLeod, Dept. of Computer Science, USC

Gleb Morein, CSE, University of California, Davis

Kazuyoshi Nanjo, CSE, UC Davis and Tohoku University, Japan

Jay Parker, Satellite Geodesy and Geodetic Systems, JPL

Marlon Pierce, Community Grids Lab, University of Indiana

Paul Rundle, Department of Physics, Harvey Mudd College; and CSE, University o f California, Davis

Robert Shcherbakov, CSE, University of California, Davis

Kristy Tiampo, Dept. of Geology, University of Western Ontario, London, Ontario

Terry Tullis, Dept. of Geology, Brown University

Don Turcotte, Dept. of Geology, University of California, Davis

(JB Rundle et al., Phys. Rev. E, v 61, p. 2416, 2000; AGU Monograph, Geocomplexity & the Physics of Earthquakes, ed. JB Rundle, DL Turcotte, W. Klein, 2000; PB Rundle et al., Phys. Rev. Lett., 87, 148501 (2001); J.B. Rundle, K.F. Tiampo, W. Klein and J.S.S. Martins, Proc. Nat. Acad. Sci. USA, 99, Supplement 1, 2514-2521, (2002))

Space-Time Patterns of Historic Earthquakes

Earthquakes on major faults occur quasi-periodically

Major events on the San Andreas Fault

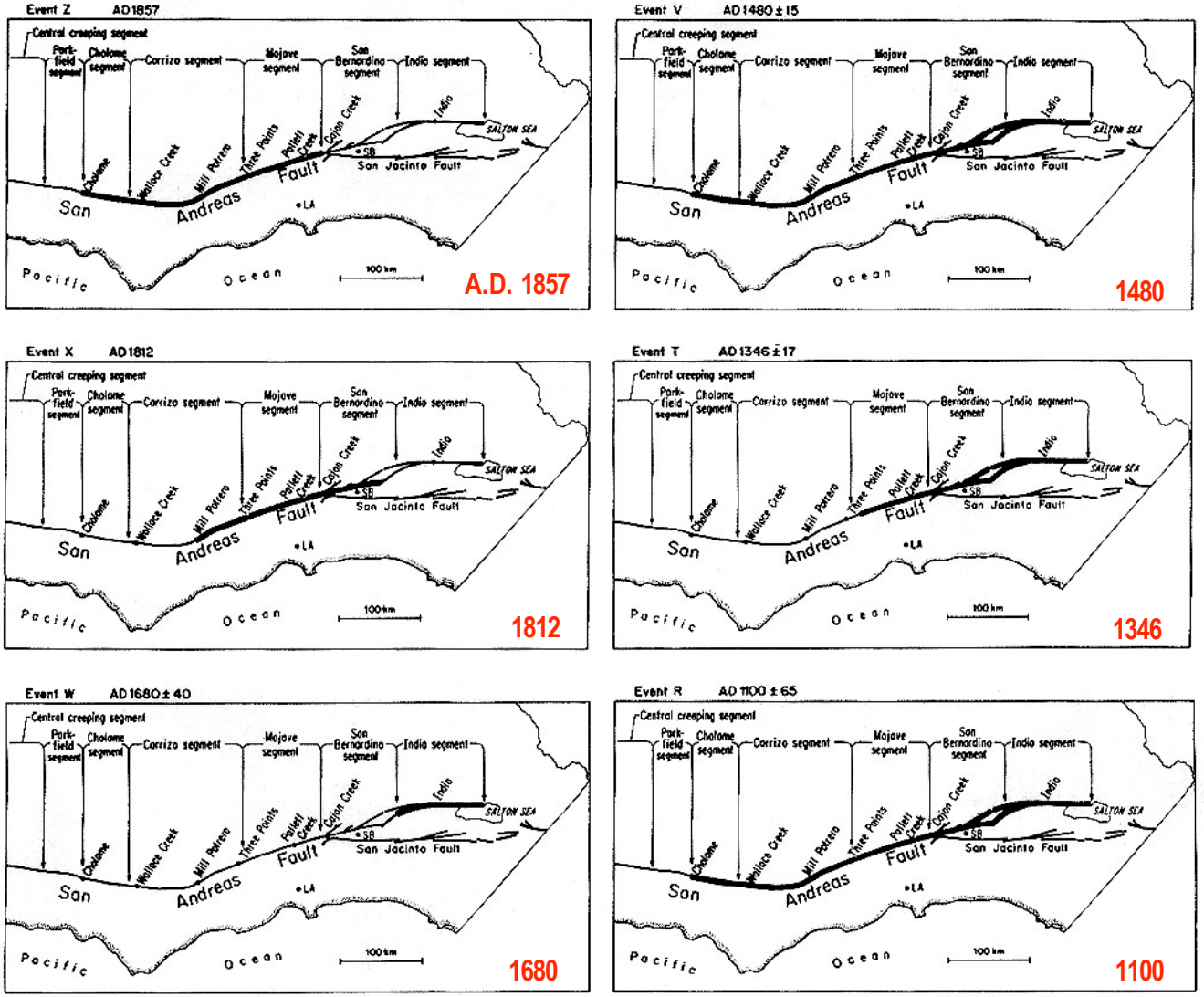

From K. Sieh et al., JGR, 94, 603 (1989)

Virtual California 2001 Represents All the Major Active Strike Slip Faults in California

(PB Rundle et al, to be submitted, 2004)

Faults in RED are shown superposed on a LandSat image of California.

(Image courtesy of Peggy Li, JPL)

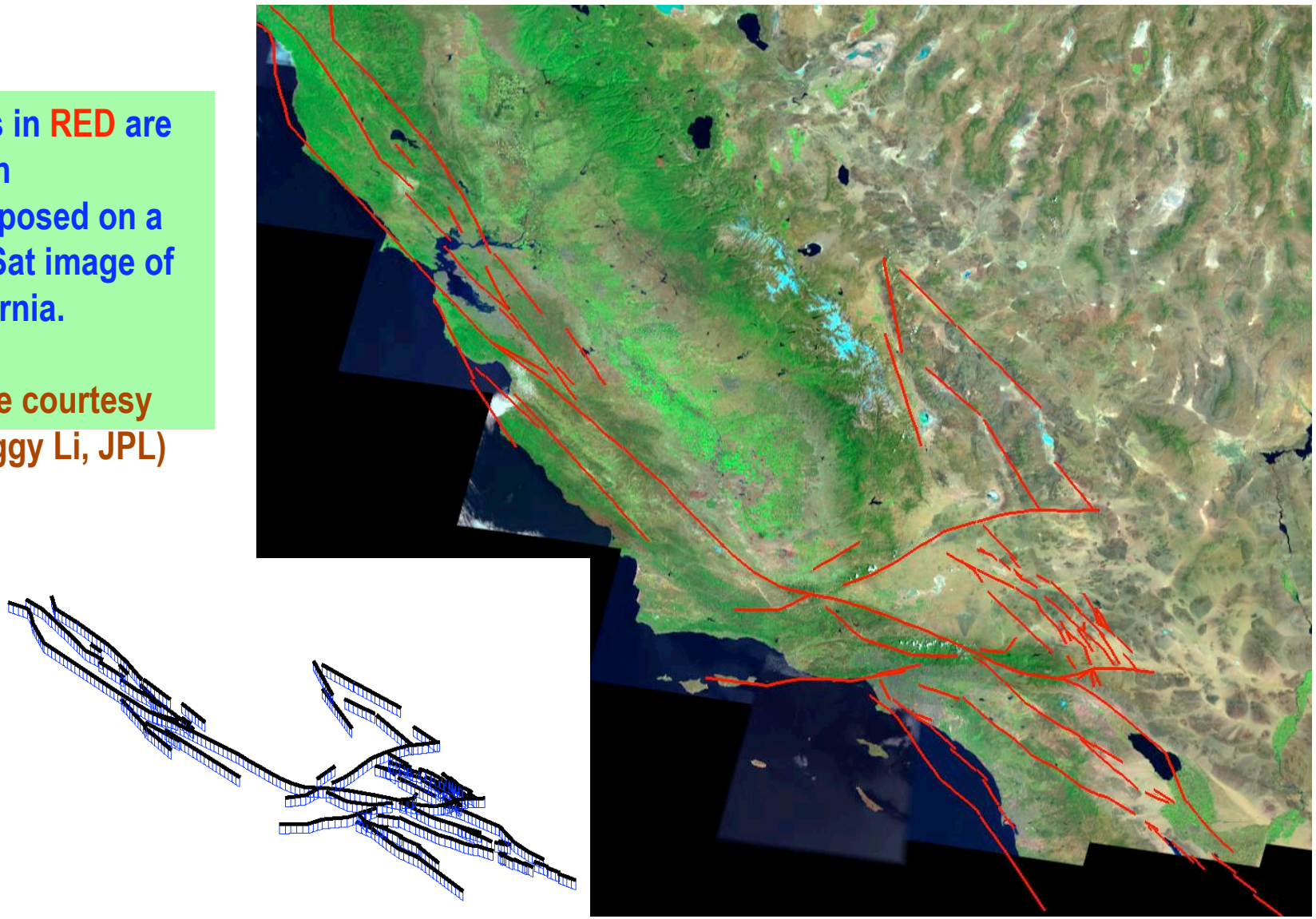

The Virtual_California Simulation:

Present Characteristics & Properties

Backslip model – Topology of fault system does not evolve. Stress accumulation occurs as a result of negative slip, or "backslip".

Linear interactions (stress transfer) - Interactions (stress Greens functions) are purely elastic.

Arbitrarily complex 3D fault system topologies -- All faults are vertical strike-slip faults. Boundary element mesh is ~ 10 km horizontal, 15 km vertical. Faults are embedded in an elastic half space.

Friction laws -- Based on laboratory experiments, and include additive stochastic noise. Method of solution for stochastic equations is therefore via Cellular Automaton methods.

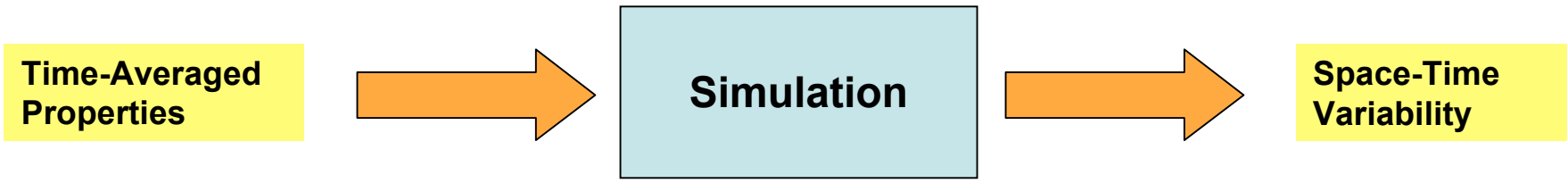

Examples of Large Single Events

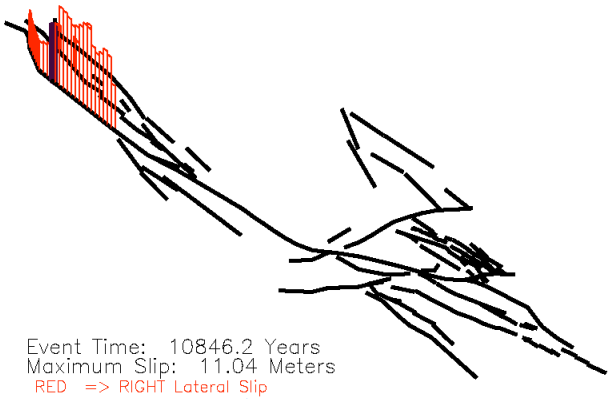

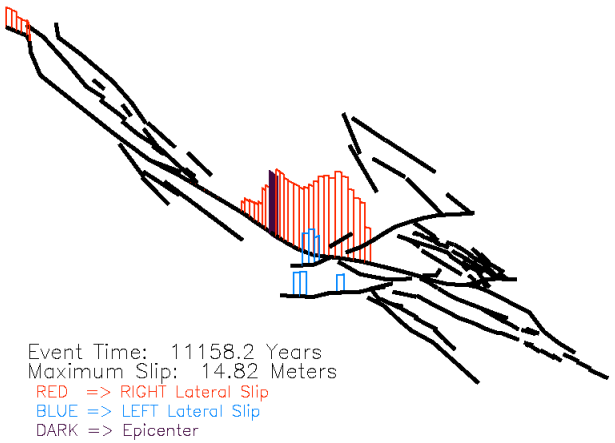

Two large events on the San Andreas Fault. The dark bar indicates the epicentral segment.

Both events are non-local. That is, slip is not only on contiguous fault segments, but slip also occurs on disjoint segments from the main group of slipped segments.

Space-Time Clustering

(Images Produced with Virtual California code by P. Li, JPL)

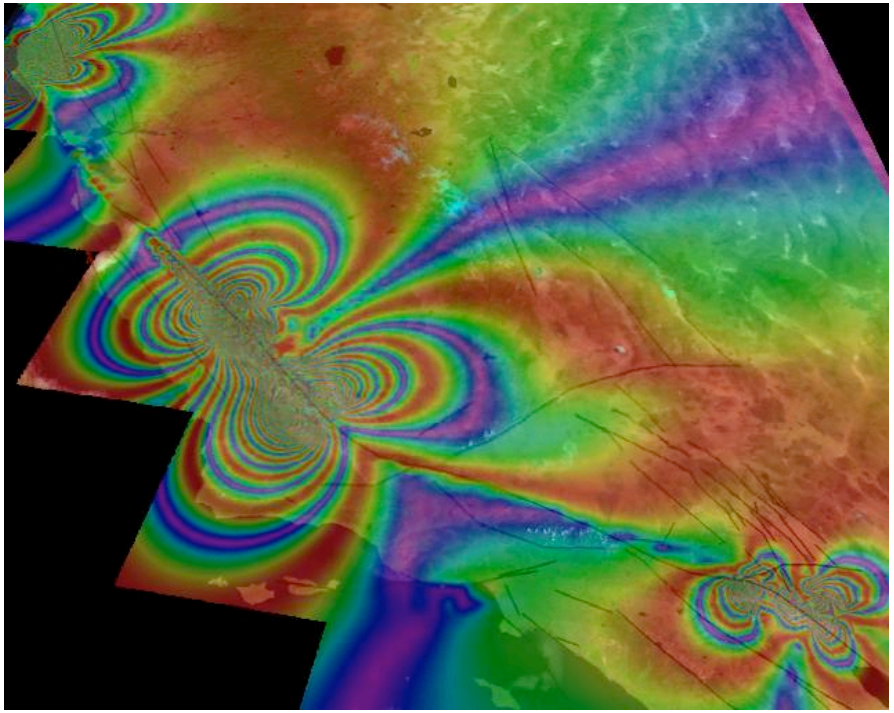

Time Index = 190

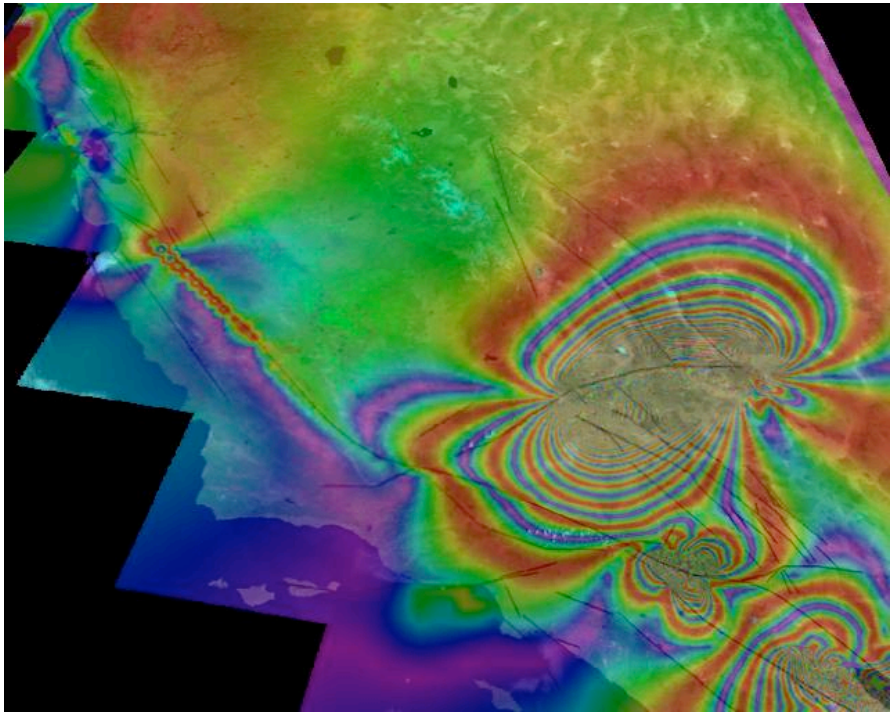

Time Index = 963

Simulation of 1000 years of California Earthquakes Obtained from System-Level Virtual California Model of Earthquake Dynamics

http://pat.jpl.nasa.gov/public/RIVA/images.html

Simulations and space-time patterns revealed by InSAR fringes

Each movie frame represents surface deformation over the previous 5 years.

Frames advance 1 year at a time. (Movie courtesy of P Li, JPL).

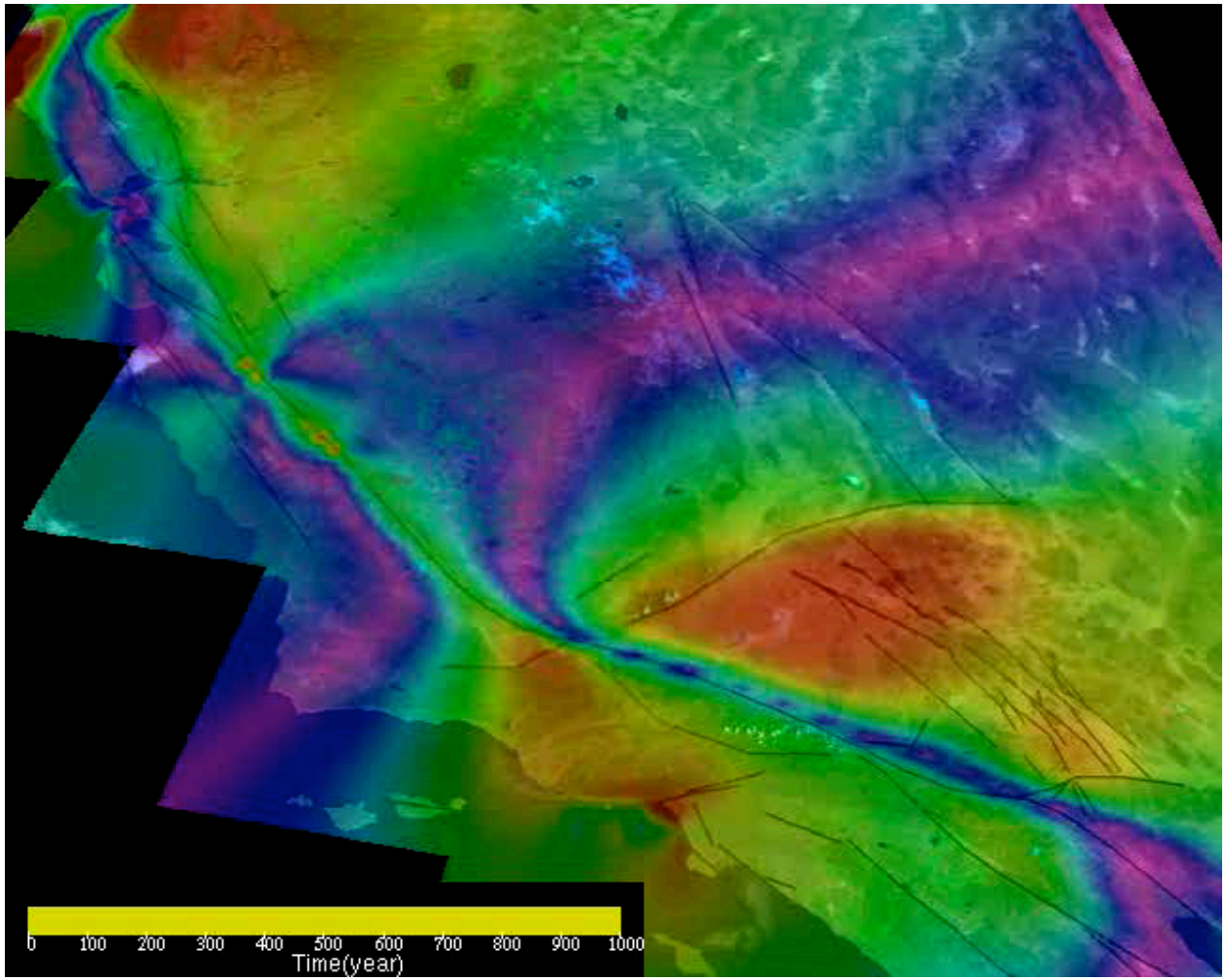

Clustering of events in space and time can be seen.

Forecasting the Next Great San Francisco Earthquake

We compute ("measure") a family of conditional probability distributions $P(T_P \mid T_F)$, which is the probability that a great earthquake of either M > 7.0 or M > 7.3 occurs on the yellow section (see map at right) of the Northern SAF at a time T_F in the future, given that no such earthquake has occurred at a time T_P since the last such event.

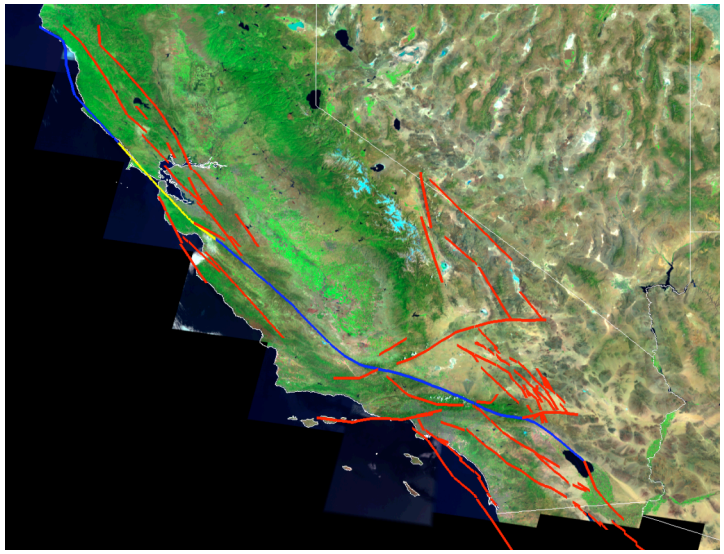

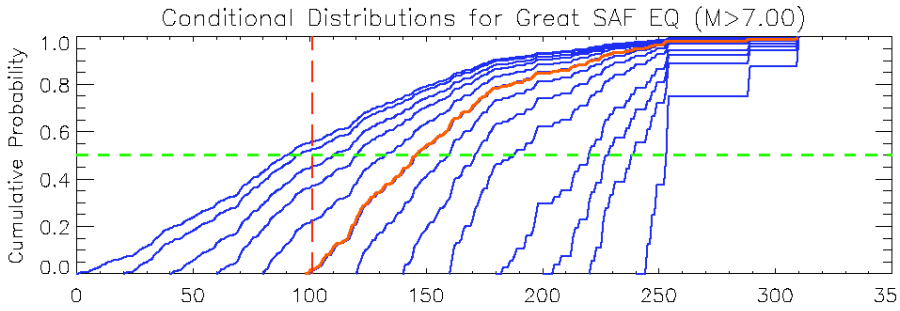

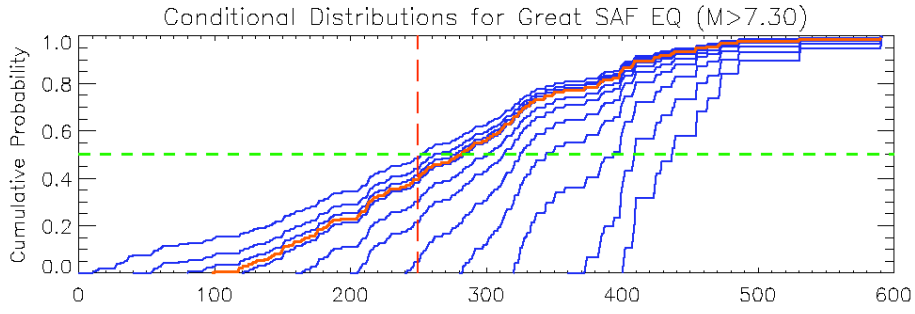

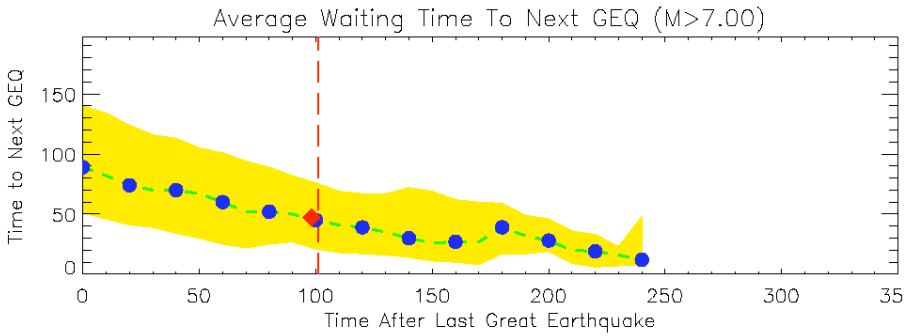

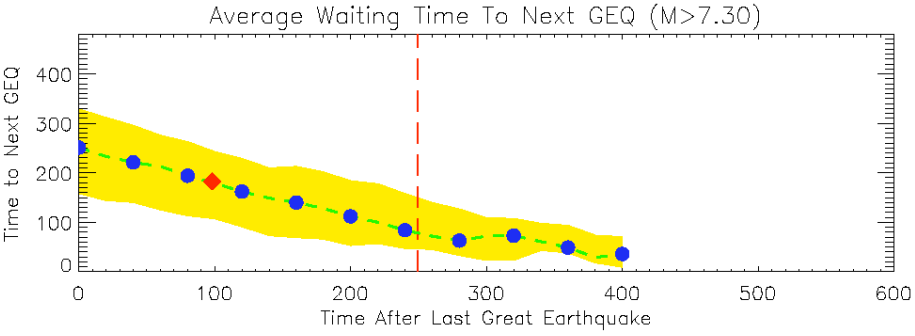

The yellow region is $.25 \le P(T_P \mid T_F) \le .75$, the middle 50%. The red diamond represents the value for today, 98.2 years after the great 1906 San Francisco earthquake. The dashed red vertical lines represent the average (mean) recurrence intervals, 101 years for m > 7.0, and 249 years for m > 7.3

Forecasting Earthquakes via Pattern Informatics ("Hotspot") Method

Earthquake activity over a period of time can be represented by a state vector $\Psi(x,t)$, which can be written as a sum over KL eigenfunctions. Differences in state vectors have been found to represent a probability measure for future activity. Method analyzes the shifting patterns of earthquakes through time.

Using Pattern Informatics to generate an earthquake forecast (2000 to ~ 2010)

1. Spatially coarse grain (tile) the region with boxes .1° x .1° on a side (~3000 boxes, ~ 2000 with at least one earthquake from 1932 to 2000). This scale is approximately the size of a M ~ 6 earthquake, although method seems to be sensitive down to a level of M ≥ 5.
2. $\Psi_1(x_i)$ ≡ Temporal average of seismic in box iactivity from 1932 to 1990 for earthquakes with M ≥ 3 averaged over 11 km x 11 km boxes
3. $\Psi_2(x_i)$ ≡ Temporal average of activity from 1932 to 2000 for earthquakes earthquakes with M ≥ 3 averaged over 11 km x 11 km boxes
4. $\Delta\Psi(x_i) = \Psi_2(x_i) - \Psi_1(x_i)$ ≡ Change in average activity, 1990 to 2000, for earthquakes with M ≥ 3 averaged over 11 km x 11 km boxes
5. Seismic Potential $\Delta P(x_i) = \{\Delta\Psi(x_i)\}^2 - \langle\{\Delta\Psi(x_i)\}^2\rangle$ ≡ Increase in probability for a earthquakes with M ≥ 3 averaged over 11 km x 11 km boxes. Symbol <> represents spatial average.
6. Color code the result. From retrospective studies, we find that $\Delta P(x_i)$ measures not only the average change in activity during 1990-2000 (triangles at right), but also indicates locations for future activity for the period ~ 2000 to 2010.
6. Green Triangles: M ≥ 5 1990-2000

(JB Rundle, KF Tiampo, W. Klein, JSS Martins, PNAS, v99, Supl 1, 2514-2521, Feb 19, 2002; KF Tiampo, KF Tiampo, JB Rundle, S. McGinnis, S. Gross and W. Klein, Europhys. Lett., 60, 481-487, 2002).

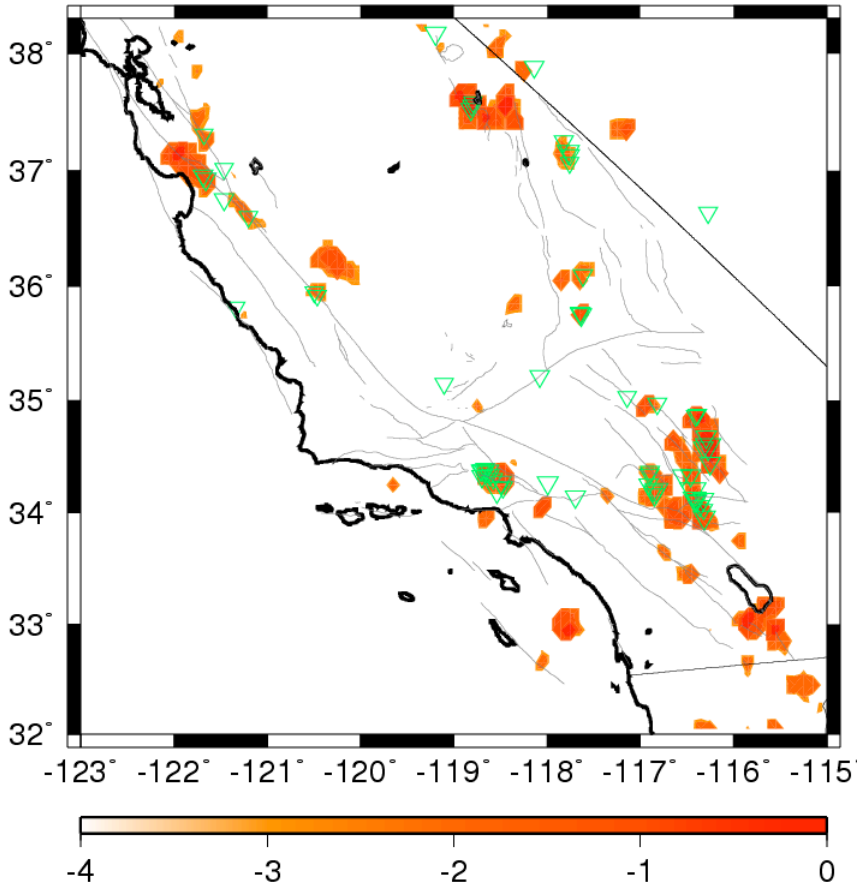

Plot of Log_{10} (Seismic Potential) for large earthquakes, M ≥ 5, ~ 2000 to 2010

Status of the Real Time Earthquake Forecast Experiment (Composite Version)

(JB Rundle et al., PNAS, v99, Supl 1, 2514-2521, Feb 19, 2002; KF Tiampo et al., Europhys. Lett., 60, 481-487, 2002; JB Rundle et al.,Rev. Geophys. Space Phys., 41(4), DOI 10.1029/2003RG000135 ,2003. http://quakesim.jpl.nasa.gov)

How are We Doing?
(Composite N-S Catalog)

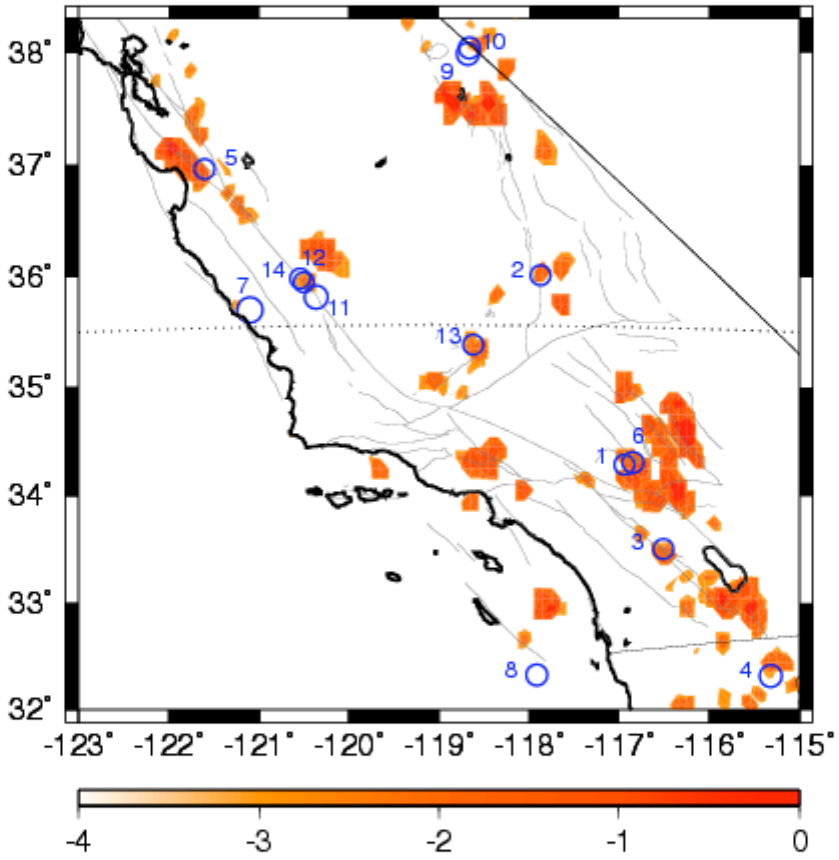

Plot of Log_{10} (Seismic Potential)

Increase in Potential for large earthquakes, M ≥ 5, ~ 2000 to 2010

Fourteen large events (blue circles) with M ≥ 5 have occurred on Central or Southern California on anomalies, or within the margin of error (+/- 11 km; Data from S. CA. and N. CA catalogs):

After the work was completed

1. Big Bear I, M = 5.1, Feb 10, 2001
2. Coso, M = 5.1, July 17, 2001

After the paper was in press (September 1, 2001)

3. Anza, M = 5.1, Oct 31, 2001

After the paper was published (February 19, 2002)

4. Baja, M = 5.7, Feb 22, 2002
5. Gilroy, M=4.9 - 5.1, May 13, 2002
6. Big Bear II, M=5.4, Feb 22, 2003
7. San Simeon, M = 6.5, Dec 22, 2003
8. San Clemente Island, M = 5.2, June 15, 2004
9. Bodie I, M=5.5, Sept. 18, 2004
10. Bodie II, M=5.4, Sept. 18, 2004
11. Parkfield I, M = 6.0, Sept. 28, 2004
12. Parkfield II, M = 5.2, Sept. 29, 2004
13. Arvin, M = 5.0, Sept. 29, 2004
14. Parkfield III, M = 5.0, Sept. 30, 2004

Note: The original forecast was made using only the Southern California catalog, which does not contain earthquakes from Central and Northern California. This composite plot was made using data from both the Northern California catalog and the Southern California catalog after the San Simeon event occurred. N. Calif. earthquake catalog is used north of dashed line, S. Calif. Catalog is used south of dashed line. Green triangles mark locations of large earthquakes between Jan 1, 1990 – Dec 31, 1999.

CL#03-2015

Note: Two events have been removed from the previous scorecard due to erroneous magnitude assignments by the USGS (Bodie I, M= 5.0 Jan 21, 2000; Parkfield II, M=5.0, Sept 28, 2004)

Forecasting Earthquake Locations in Japan: Kobe Area

JMA Catalog is used. Several variations of the basic method, which differ in the order that operations are applied, are compared below (K. Nanjo, JB Rundle, J Holliday, DLT, 2004)

Forecast for the period:
January 1, 2000 ~ December 31, 2010

Parameters used: t_0 = Jan. 1, 1970; t_1 = Jan. 1, 1990; t_2 = Dec. 31, 1999 (Latitudes: 32.9-36.4; Longitudes: 133.0-137.0) Triangles: Large events having M ≥ 5 during $t_1 \le t \le t_2$. Circles: Large events having M ≥ 5 during $t > t_2$. Events are used from the surface to 20 km below the surface. All events having M ≥ 3 in the catalog are used.

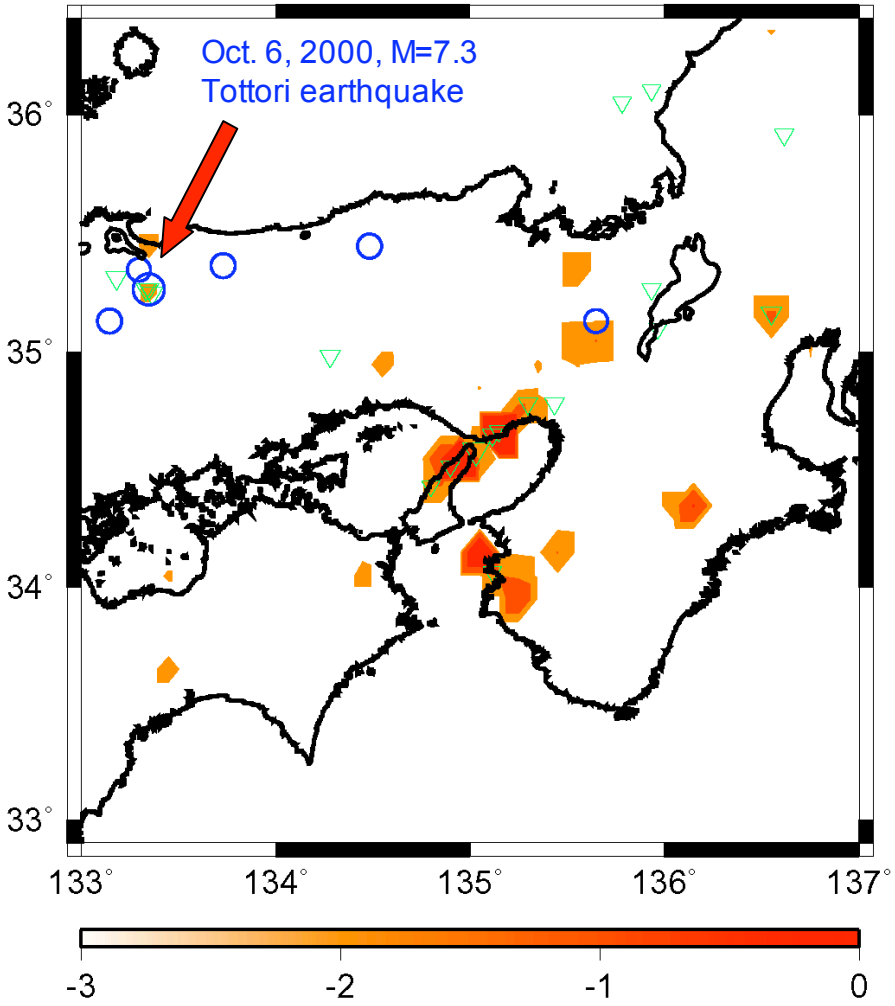

Forecasting Earthquake Locations in Japan: Tokyo Area

JMA Catalog is used. Several variations of the basic method, which differ in the order that operations are applied, are compared below (K. Nanjo, JB Rundle, J Holliday, DLT, 2004)

Forecast for the period:
January 1, 2000 ~ December 31, 2010

Parameters used: t_0 = Jan. 1, 1980; t_1 = Jan. 1, 1990; t_2 = Dec. 31, 1999 (Latitudes: 32.9-36.4; Longitudes: 133.0-137.0) Triangles: Large events having M ≥ 5 during $t_1 \le t \le t_2$. Circles: Large events having M ≥ 5 during $t > t_2$. Events are used from the surface to 20 km below the surface. All events having M ≥ 3 in the catalog are used.

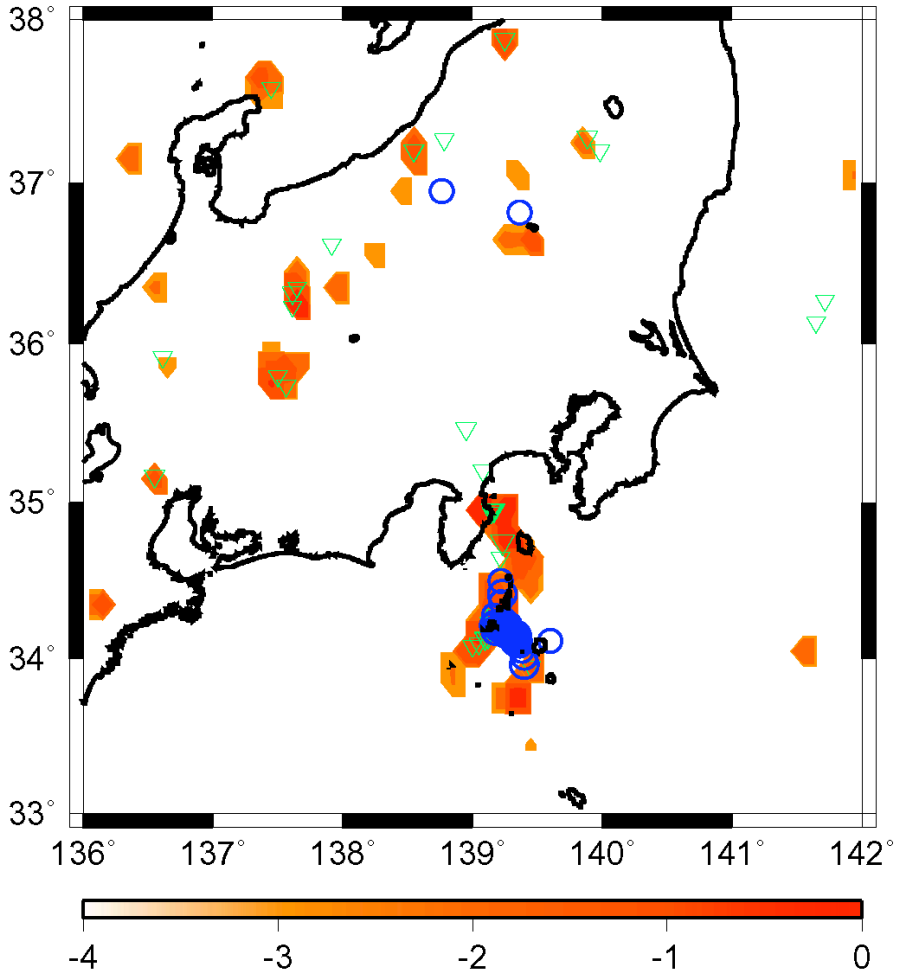

Summary

Numerical simulations like Virtual California can help us understand the system-level physics of earthquakes because:

- The effects of *complex interactions* among faults in the system are difficult to understand without a topologically realistic model

- *Many scales* in space and time are *strongly coupled*, and comprehensive observations cannot be made that can span all these scales

- Simulations allow us to relate the *observed space-time earthquake patterns*, obtained from seismicity and InSAR observations, to underlying stress and strain

Forecasting and prediction:

- Is strongly affected by the many complex *interactions* among faults in the system

- Can be facilitated by using simulations to generate *probability density functions* for use in developing forecast methods

- *Hotspot maps* can be constructed that indicate likely locations for future earthquakes with $M \geq 5$, utilizing techniques that originated with methods to forecast El Nino-Southern Oscillation

Is This Apparent Agreement an Accident?

Computing the Probability that the Apparent Agreement in Location is due to Random Chance – 3 Computations

A Simplistic Analysis Based on the Binomial Distribution

1. Conditions: 14 large events, 13 lie on hotspots or within margin of error (+/- 11 km). Probability of a hit is assumed proportional to percentage of active area of enlarged hotspots ~ .24 (figure as per M. Blanpied, USGS).

2. Conditions: 14 large events, 8 “hits” within actual hotspots, 6 “misses” (estimates from R. Stein, USGS & JBR). Probability of a hit is assumed proportional to percentage of active area of hotspots ~ ..09 (figure as per M. Blanpied).

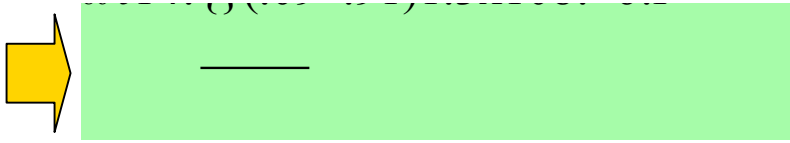

3. Conditions: 10 mainshock-foreshocks groups of large events. 9 occur in association with an enlarged hotspot. Probability of a hit is assumed proportional to percentage of active active area of enlarged hotspots ~ .24 (figure as per M. Blanpied).